Affinity and Sequence Specificity of DNA Binding and Site Selection for Primer Synthesis by *Escherichia coli* Primase†

Sujata Khopde,‡ Esther E. Biswas,‡,§ and Subhasis B. Biswas*,‡

Department of Molecular Biology, School of Osteopathic Medicine, and Graduate School of Biomedical Sciences, University of Medicine and Dentistry of New Jersey, Stratford, New Jersey 08084, and Program in Biotechnology, Department of Laboratory Sciences, Thomas Jefferson University, Philadelphia, Pennsylvania 19107

Received August 23, 2002; Revised Manuscript Received October 7, 2002

ABSTRACT: Primase is an essential DNA replication enzyme in *Escherichia coli* and responsible for primer synthesis during lagging strand DNA replication. Although the interaction of primase with single-stranded DNA plays an important role in primer RNA and Okazaki fragment synthesis, the mechanism of DNA binding and site selection for primer synthesis remains unknown. We have analyzed the energetics of DNA binding and the mechanism of site selection for the initiation of primer RNA synthesis on the lagging strand of the replication fork. Quantitative analysis of DNA binding by primase was carried out using a number of oligonucleotide sequences: oligo$(dT)_{25}$ and a 30 bp oligonucleotide derived from bacteriophage G4 origin (G4ori-wt). Primase bound both sequences with moderate affinity ($K_d = 1.2-1.4 \times 10^{-7}$ M); however, binding was stronger for G4ori-wt. G4ori-wt contained a CTG trinucleotide, which is a preferred site for initiation of primer synthesis. Analysis of DNA binding isotherms derived from primase binding to the oligonucleotide sequences by fluorescence anisotropy indicated that primase bound to DNA as a dimer, and this finding was further substantiated by electrophoretic mobility shift assays (EMSAs) and UV cross-linking of the primase−DNA complex. Dissection of the energetics involved in the primase−DNA interaction revealed a higher affinity of primase for DNA sequences containing the CTG triplet. This sequence preference of primase may likely be responsible for the initiation of primer synthesis in the CTG triplet sites in the *E. coli* lagging strand as well as in the origin of replication of bacteriophage G4.

DNA primase of *Escherichia coli* is a specialized single-stranded DNA-dependent RNA polymerase, which synthesizes small RNA primers during replication of the *E. coli* genome and encoded by the dnaG gene (*1*). In the replication fork, DnaB helicase unwinds the DNA duplex and allows primase to initiate primer synthesis on both leading and lagging strands (*2*, *3*). Primase is required for synthesis of RNA primers only once on the leading strand and repeatedly on the lagging strand in the formation of Okazaki fragments.

Previous studies with primase indicated that the RNA primers synthesized by primase begin with the pppAG dinucleotide at the 5′ end (*4*−*7*). G4 origin has been extensively used as a model system to analyze primase action (*1*, *7*). In vitro studies have demonstrated that none of the three hairpin regions, normally present in G4 origin, are required for the primase action, but the CTG trinucleotide sequence is essential (*1*, *7*). In addition, primase initiates in vivo Okazaki fragment synthesis of *E. coli* chromosome and λ-bacteriophage predominantly from unique regions containing trinucleotide CTG and synthesizes the diribonucleotide 5′-pppApG-3′ primer (*8*, *9*).

Unlike DnaB helicase, primase has distributive action in Okazaki synthesis. It does not associate for the long term with the replication fork, and a new molecule of primase is required for every new primer synthesis on each Okazaki fragment (*10*). The length of the fragment is inversely related to the primase concentration (*11*). Association of primase with ssDNA is the key event in the Okazaki cycle. The kinetics of primer synthesis catalyzed by primase using a 23-nucleotide DNA template have been studied. The incorporation of first two nucleotides is very slow as compared to incorporation of the next 10 nucleotides, suggesting that the rate-determining step is either the formation of the first phosphodiester bond or some step preceding it (*12*). Consequently, primase binding to ssDNA template may play an important role in the rate and extent of primer synthesis. However, quantitative analysis of the interaction of primase with DNA has not been carried out, making it difficult to understand the mechanism that triggers the initiation of primer synthesis at the CTG trinucleotide sequence.

Primase is a monomer in solution (*13*). However, most replication proteins are oligomeric in nature (*14*, *15*), or they form doughnut-shaped oligomers in the presence of ssDNA[1] (*16*, *17*). Many DNA binding proteins form higher oligomeric

† This work was supported by a grant from the National Institute of General Medical Sciences, National Institutes of Health (GM36002), and funds from the University of Medicine and Dentistry of New Jersey.

* To whom correspondence should be addressed. Telephone: (856) 566-6270. Fax: (781) 207-8476. E-mail: biswassb@umdnj.edu.

‡ University of Medicine and Dentistry of New Jersey.

§ Thomas Jefferson University.

[1] Abbreviations: Tris, tris(hydroxymethyl)aminomethane; BSA, bovine serum albumin; EDTA, ethylenediaminetetraacetic acid; ssDNA, single-stranded DNA; EMSA, electrophoretic mobility shift assay; DTT, dithiothreitol; wt, wild type.

10.1021/bi026711m CCC: $22.00 © 2002 American Chemical Society
Published on Web 11/20/2002

Table 1: Alignment of DNA Sequences from the Origins of Replication of G4, ϕK Bacteriophages, R1, and R6K Plasmids along with Synthetic DNA Template Sequences Used in the Binding Experiments

Templates	Sequences
	Primer RNA
	ppp A G . . .
	-11 -1 + 1
G4 [a]	3'-A **A** A **C G T C** A T C C C T G C C G C **C** G-5'
ϕK [a]	3'-A **A** T **C G T C** C T C C C T T C C G C **C** G-5'
R1 [a]	3'-G **A** C **C G T C** C C C G A C C C C T A **C** C-5'
R6K [a]	3'-G **A** C **C G T C** C C C C G C G T T C G **C** G-5'
	Unlabeled G4 sequences
G4ori-wt	3'-A G G A A A A C C G A **A** A **C G T C** A T C C C T G C C G C **C** G-5'
G4ori-mut1	3'-A G G A A A A C C G A ***T*** A **C G T C** A T C C C T G C C G C **C** G-5'
G4ori-mut2	3'-A G G A A A A C C G A **A** A ***T T*** **T C** A T C C C T G C C G C **C** G-5'
G4ori-mut3	3'-A G G A A A A C C G A **A** A **C G T** ***T*** A T C C C T G C C G C **C** G-5'
	5'-Fluorescein labeled sequences
Fl-G4ori	3'-A G G A A A A C C G A **A** A **C G T C** A T C C C T G C C G C **C** G-**Fluorescein**-5'
Fl-(dT)$_{25}$	3'-T T T T T T T T T T T T T T T T T T T T T T T T T-**Fluorescein**-5'

[a] From ref *1*.

structure in the nucleoprotein complex (*18*, *19*). These structures appear to help these proteins stay loosely bound to the DNA that is being replicated, allowing them to act like mobile replication promoters (*20*) unlike transcription factors, which grip DNA and remain tightly bound. Consequently, it is perhaps possible that replication proteins, in general, bind DNA in a manner that is distinct from that of DNA binding proteins such as transcription factors that stay bound to the target sequence. Recent X-ray crystallographic studies of the catalytic domain of primase have been reported, but they did not demonstrate any oligomeric structure or the exact nature of the DNA binding site (*21*). However, even though primase exists essentially as a monomer in solution, it has been shown that a 1:1 complex of primase and G4 circular ssDNA failed to promote primer synthesis, but addition of primase to increase the ratio to 2:1 resulted in primer synthesis (*22*). To fully delineate the interactions of primase with the single-stranded DNA template, we have characterized the binding affinity of primase with a variety of CTG-less and CTG-containing templates derived from G4 bacteriophage.

The fluorescence anisotropy analysis of protein−DNA interaction is a very convenient, quantitative, and rapid method for direct assessment of binding in solution under a variety of experimental conditions (*23*−*28*). More importantly, this methodology does not require separation of the complex from the free ligand or immobilization of the ligand to a surface. The utility of this method has been clearly demonstrated in studying protein−DNA interactions involving a number of DNA binding proteins, e.g., estrogen receptor binding to estrogen responsive elements by Royer and co-workers (*26*, *27*). Consequently, this method is ideal for a detailed analysis of DNA−protein interaction involving DNA primase. However, we have used a combination of fluorescence anisotropy with an electrophoretic mobility shift assay (EMSA) and ultraviolet cross-linking of the protein−DNA complex to analyze primase−DNA interaction. The energetics involved in the formation of the primase−DNA complex were evaluated by analyzing the anisotropy data using a computer algorithm, BIOEQS, developed by Royer et al., that is designed for analysis of biological equilibrium processes such as ligand binding (*26*−*28*).

MATERIALS AND METHODS

Nucleic Acids, Enzymes, and Other Reagents. The pRLM96 plasmid was a kind gift of R. McMacken of Johns Hopkins University (Baltimore, MD). The DnaG primase gene was subcloned from pRLM96 into the T7 expression vector, pET29b (Novagen Inc., Madison, WI), using *Bam*HI and *Hin*dIII restriction enzymes. The resultant plasmid was termed pET29b-DnaG. Labeled and unlabeled oligonucleotides were purchased from Sigma-Genosys (Pittsburgh, PA). Labeled oligonucleotides were covalently linked with the fluorescein probe at the 5′ end during oligonucleotide synthesis.

The following unlabeled oligonucleotides were used: oligo(dT)$_{25}$, oligo(dT)$_{20}$, oligo(dT)$_{15}$, oligo(dC)$_{15}$, oligo(dA)$_{15}$, oligo(dT)$_{10}$, and oligo(dT)$_6$. Mutated oligonucleotide sequences of G4 are presented in Table 1. All other reagents used in this study were ACS reagent or spectroscopy grade and obtained from Aldrich Chemical Co. (Milwaukee, WI). HPLC grade water was obtained from Fisher Chemicals (Pittsburgh, PA) and analyzed for low autofluorescence.

Buffers. Buffer A was 25 mM Tris-HCl (pH 7.5), 1 mM EDTA, 5 mM Mg^{2+}, 5 mM DTT, and 10% glycerol. Lysis buffer was 25 mM Tris-HCl, 10% sucrose, and 250 mM NaCl. Buffer B contained 20 mM Tris-HCl (pH 7.5), 10% glycerol, 5 mM Mg^{2+}, and 1 mM DTT (KCl as indicated).

Primase Expression and Purification. Primase was overexpressed in the *E. coli* BL21 (DE3, p*Lys*S) strain harboring the pET29b-DnaG expression plasmid. *E. coli* cells were grown in 6 L batches in 2×YT medium containing 50 μg/mL kanamycin at 37 °C to an OD_{600} of 0.4. At this stage, 1-isopropyl 1-thio-β-D-galactopyranoside (IPTG) was added to a final concentration of 0.25 mM. The culture was grown for additional 3 h. Cells were harvested at 4000*g* for 10 min, and the cell pellet was resuspended in lysis buffer. The cells were lysed with 0.2 mg/mL lysozyme, 5 mM $MgCl_2$, 5 mM DTT, and protease inhibitors by incubating them on ice for 60 min followed by incubation at 37 °C for 15 min. This mixture was then chilled on ice, and 2 mM spermidine hydrochloride was added. The cells were sonicated and incubated with 0.5 M sodium chloride for 1 h on ice while being shaken.

The lysate was centrifuged at 40000*g* and 4 °C for 30 min. The supernatant was precipitated with 0.3 g/mL ammonium sulfate on ice for 1 h followed by centrifugation. The pellet was resuspended in buffer A and dialyzed overnight to adjust the conductivity to that of buffer A10 (buffer A with 10 mM NaCl). The protein was loaded on a 20 mL POROS HQ column (Applied Biosystems Inc., Foster City, CA) pre-equilibrated with buffer A10 followed by washing with the same. The protein was eluted using a linear 40 mL gradient each of buffer A10 → buffer A500 at a flow rate of 1 mL/min. The peak fractions were identified, pooled, and purified further by HPLC gel filtration chromatography on a 2 cm × 60 cm ToyoSoda TSK250 column obtained from Bio-Rad (Richmond, CA) on a BIOCAD-20 HPLC system (Applied Biosystems Inc.). The flow rate was 2 mL/min, and the elution buffer was buffer A containing 150 mM NaCl. The peak fractions were identified, collected, and concentrated by ammonium sulfate precipitation. The protein that was obtained was almost ~95% pure (Figure 1A). The protein homogeneity was determined by using SDS gel electrophoresis, and the protein concentration was determined by the method of Bradford (*29*). The concentration of purified primase was determined by UV absorption at 280 nm using a molar extinction coefficient of 47 800 M^{-1} cm^{-1} (*12*).

Steady State Fluorescence Measurements. Fluorescence experiments were performed on a Perkin-Elmer LS50B spectrofluorometer (Perkin-Elmer Inc., Shelton, CT) or a photon-counting spectrofluorometer equipped with a Hamamatsu R928P photomultiplier tube, and the measurements were taken in an L format. Excitation and emission slits were adjusted to 8 and 4 nm, respectively.

The 5′-fluorescein-labeled oligonucleotides {oligo$(dT)_{25}$ [Fl-$(dT)_{25}$] and G4ori-wt (Fl-G4ori)} were used as fluorescence anisotropy probes (Table 1). They were diluted in buffer B to a concentration of 3 nM and titrated with primase in the concentration range of 0.1 nM to 1 μM. The samples were excited at 488 nm, and the fluorescence anisotropy was measured at 540 nm (*23*−*25*), where minimal variation in the total fluorescence intensity was observed. The temperature was adjusted by using a thermostat attached to the cell chamber. Fluorescence intensities were measured for 3 × 10 s and averaged. Anisotropy values were expressed as millianisotropy (mA), which is equal to the anisotropy divided by 1000. The standard deviation for the anisotropy values was <2 mA. The total fluorescence intensity did not change significantly with an increase in primase concentration as shown in Figure 2B. Therefore, the anisotropy measurements were not affected by the fluorescence lifetime changes or the scattered excitation light.

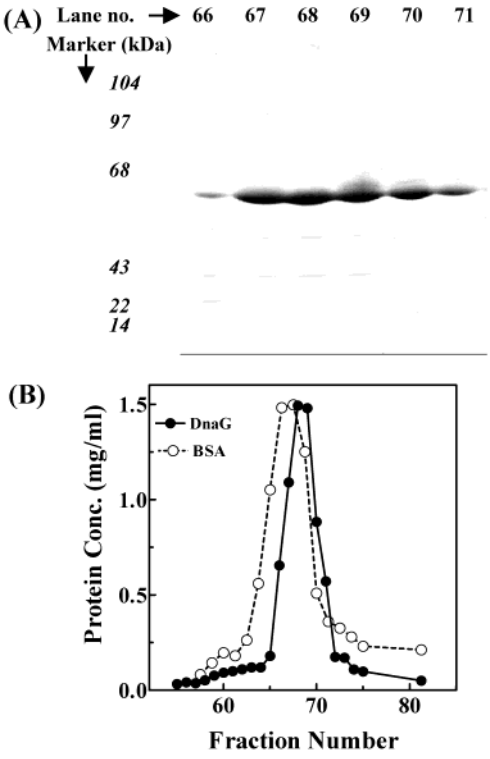

FIGURE 1: Purification of *E. coli* primase. (A) SDS−PAGE analysis of purified primase obtained after the gel filtration purification step. (B) Gel filtration chromatography of (●) primase and (○) bovine serum albumin (BSA). The column was Bio-Rad TSK 250 (2.2 cm × 60 cm) high-resolution, preparative HPLC gel filtration column fitted to a BIOCAD-20 (Applied Biosystems Inc.) HPLC system maintained at 4 °C. The flow rate was 2 mL/min. The protein concentration was checked by the method of Bradford (*29*).

Analysis of the Fluorescence Anisotropy Data. The interaction of primase with labeled oligonucleotide can be represented as follows:

$$R + P \leftrightarrow RP \quad (1)$$

where R is a ligand, i.e., labeled oligonucleotides, and P is primase, the concentration of which was varied during titration.

At equilibrium, K_a, the equilibrium association constant, can be given as

$$K_a = [RP]/([R][P]) \quad (2)$$

$$K_a[R][P] = [RP] \quad (3)$$

The fraction of the binding sites occupied can be represented as

$$f = [\text{occupied binding sites}]/[\text{total binding sites}] = [RP]/([R] + [RP]) \quad (4)$$

Substituting for [RP] and rearranging the equation, we obtain

$$f = K_a[P]/(1 + K_a[P]) \quad (5)$$

$$f = [P]/([P] + 1/K_a) \quad (6)$$

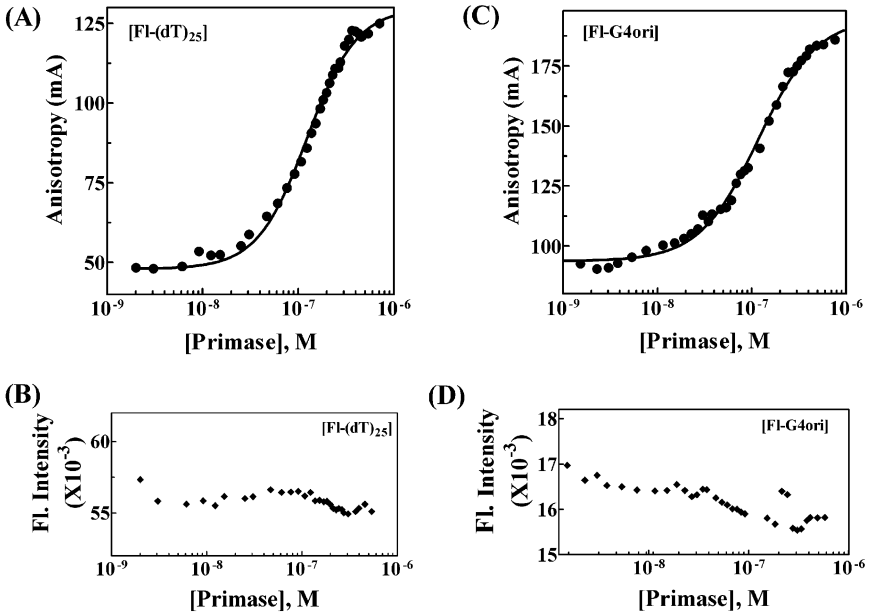

FIGURE 2: Fluorescence anisotropy analysis of primase−oligo(dT)$_{25}$ and primase−Fl-G4ori interactions. (A and B) Titration of 3 nM Fl-(dT)$_{25}$ with primase at 23 °C in buffer B containing 25 mM KCl: (A) fluorescence anisotropy (●) and (B) fluorescence intensity (◆) recorded at each point. (C and D) Titration of 3 nM Fl-G4ori with primase at 23 °C in buffer B containing 25 mM KCl: (C) fluorescence anisotropy (●) and (D) fluorescence intensity (◆) recorded at each point. Nonlinear regression fits by GraphPad Prism3.01 are represented with lines.

Similarly, the equilibrium dissociation constant K_d ($K_d = 1/K_a$) can be expressed as

$$f = [P]/([P] + K_d) \quad (7)$$

at

$$f = 0.5 \text{ and } K_d = [P] \quad (8)$$

Thus, K_d can be further defined as the protein concentration at which half of the sites are occupied when the ligand concentration is constant as in the present case or the ligand concentration at which half of the sites are occupied when the protein concentration is constant. Nonlinear regression analysis of the anisotropy data was carried out using Prism 3.01 software (GraphPad Software Inc., San Diego, CA), and the K_d values, i.e., the concentrations of primase required to bind 50% of the oligonucleotides, were computed using the following equation

$$Y = A_{min} + (A_{max} - A_{min})/(1 + 10^{(X_0 - X)n_{app}}) \quad (9)$$

where A_{min} and A_{max} are the anisotropy values at the bottom and top plateaus, respectively, X represents the log of the primase concentration, X_0 is the X value when the response is halfway between the top and the bottom, and n_{app} is the Hill coefficient.

Inhibition Assays. Competition binding experiments were used to compare the binding affinities of oligonucleotides of different sequences, where a preformed primase·Fl-(dT)$_{25}$ complex was titrated with unlabeled oligonucleotides. The complex was formed by combining 3×10^{-9} M Fl-(dT)$_{25}$ and the primase at 2×10^{-7} M, which was slightly higher than the K_d. The decrease in anisotropy was monitored with the increase in competitor concentration, and data were analyzed by using a nonlinear least-squares regression algorithm. The IC_{50} values, i.e., the concentrations of unlabeled ligand required to displace half of the Fl-(dT)$_{25}$ from the complex, were computed from the regression analysis. The inhibition constant K_i is given as

$$K_i = IC_{50}/(1 + R_T/K_d) \quad (10)$$

where R_T is the total concentration of the Fl-(dT)$_{25}$. Since it is negligible in comparison to the K_d, the IC_{50} is equivalent to the inhibition constant, K_i.

BIOEQS Analysis. Anisotropy data were also analyzed by using the BIOEQS program following the instruction of C. Royer (*26*−*28*). This program takes into account the different oligomeric states of proteins involved in each step of the reaction and, thus, analyzes more complex binding models than standard nonlinear regression algorithms. On the basis of the concentrations of the protein and ligand and the final stoichiometries, this program derives the free energy involved in the formation of each postulated DNA−protein complex species. The details of this program have been described previously (*26*−*28*).

Since the final stoichiometry of the primase−DNA interaction is not known exactly, both a simple binding model and a sequential dimer model were tested for their ability to describe the interaction of primase with the DNA. The simple binding model does not discriminate between one primase monomer and two noninteracting monomers of equal affinity binding to the DNA. The sequential dimer model describes the DNA binding of two primase proteins that interact with each other. This model incorporates free DNA, free primase monomer, primase monomer-bound DNA, and primase dimer-bound DNA, but not a free dimer. The plateau values of anisotropy were floating parameters, while the anisotropy corresponding to the intermediate monomer-bound species was fixed at a value approximately halfway between two plateaus. Thus, the cooperative dimer binding model gives two free energy values ($\Delta G°_1$ and $\Delta G°$) where the first one

is for monomer DNA binding and the second one is the total free energy involved in the formation of the final complex.

The energy for the cooperativity of the interaction between two primase molecules, if any, can be obtained as follows

$$\Delta G^\circ_c = \Delta G^\circ - 2\Delta G^\circ_1 \quad (11)$$

Electrophoretic Mobility Shift Assay. The G4ori-wt sequence was labeled using [γ-^{32}P]ATP and T4 polynucleotide kinase. One nanogram of 5′-^{32}P-labeled G4ori-wt oligonucleotide was incubated with the indicated amount of primase for 10 min at room temperature in the presence of 10 mM Tris (pH 7.5), 1 mM ATP, 5 mM Mg^{2+}, 100 μM EDTA, 10% glycerol, 1 mM DTT, and 0.24 μg/mL bovine serum albumin. The final reaction volume was 20 μL. The samples were mixed with 5 μL of loading buffer containing TBE buffer [0.1 M Tris, 0.1 M boric acid, and 2 mM EDTA (pH 8)], 50% glycerol, and 0.1% bromophenol blue and electrophoresed in an 8% nondenaturing polyacrylamide gel, equilibrated with TBE buffer. Following electrophoresis, the gel was dried and subjected to autoradiography. The autoradiogram was scanned, and the intensities of the bands, which correspond to the free and bound DNA, were measured in each lane by densitometry using a digital autoradiography image analysis program from Eastman Kodak Co. (Rochester, NY). The K_d value was expressed as the protein concentration at which 50% of the DNA was in the bound form.

Ultraviolet Cross-Linking of the DNA−Protein Complex (30). Four nanograms of 5′-^{32}P-labeled G4ori-wt oligonucleotide was mixed with varying concentrations of primase and incubated at room temperature for 10 min. The samples were UV irradiated using a UV lamp (1.5 mJ/s at 254 nm) at 0 °C for 20 min. Following irradiation, the samples were collected in tubes and denatured in SDS−PAGE buffer at 100 °C for 5 min. The protein−DNA complexes were separated on a 5 to 12.5% polyacylamide gradient gel, equilibrated with SDS buffer. The gel was stained with Coomassie blue R-250. Before autoradiography was carried out, the gel was washed with 5% glycerol to remove traces of ethanol and dried under vacuum. The apparent molecular mass of the DNA−protein complex was determined by comparing its mobility with that of the standard protein marker.

RESULTS

E. coli Primase Is a Monomer in Solution. We have overexpressed primase from the pET29b-DnaG plasmid (Figure 1A) for structure−function characterization. The protein was purified to near homogeneity by POROS-Q column chromatography followed by high-performance liquid chromatography gel filtration. Following gel filtration, the fractions containing primase were homogeneous (fractions 66−73, Figure 1A,B). In HPLC gel filtration chromatography, BSA appeared to comigrate with primase, indicating that primase is a monomer in solution. As shown in the chromatogram in Figure 1B, BSA and primase almost coeluted in gel filtration analysis. These results confirm that primase exists as a monomer in solution even at high primase concentrations. We have determined that the purified primase preparation was ≥90% active in ssDNA binding by ssDNA cellulose chromatography and in vitro priming assays (data not shown).

Interactions of Primase with Single-Stranded DNA. We have analyzed the mechanism of DNA binding by primase using oligonucleotides of defined sequences labeled with a 5′-fluorescein moiety and fluorescence anisotropy. The binding constant for the interaction of DNA with primase was determined using 5′-flourescein-labeled 25 bp oligo-$(dT)_{25}$ [Fl-$(dT)_{25}$] (Table 1). Unless otherwise indicated, all anisotropy measurements were carried out in buffer B containing 3 nM fluorescein-labeled oligonucleotide and 25 mM KCl at 23 °C. Fluorescence anisotropy was measured at increasing concentrations of primase until saturation in anisotropy was observed. A semilog plot of the anisotropy values at various primase concentrations generated the binding isotherm shown in Figure 2A. The fluorescence anisotropy of Fl-$(dT)_{25}$ alone was 40 ± 2 mA. With addition of primase, the anisotropy value increased which was due to an increase in the concentration of the primase·Fl-$(dT)_{25}$ complex as shown in Figure 2A. A sigmoidal binding isotherm with a plateau at 125 mA at high primase concentrations was observed (Figure 2A). The K_d for the primase·Fl-$(dT)_{25}$ complex was 1.4×10^{-7} M.

Primase preferentially initiates primer synthesis from the CTG sequence in a number of prokaryotic priming systems, although the mechanism of this preference remains unknown (*1*, *9*). Replication origin sequences derived from different organisms contain the CTG sequence with an invariant adenine residue in the proximity (Table 1). The 5′-fluorescein-labeled wild-type G4 origin sequence (Fl-G4ori) consisting of 30 base pairs, of which 13 bases were at the 5′ end and 14 bases were at the 3′ end, flanking the CTG sequence (Table 1) was used to analyze its affinity of binding with the primase.

The binding constant of Fl-G4ori and primase was determined by anisotropy measurements, and is similar to that described earlier for oligo$(dT)_{25}$. In the absence of primase, the anisotropy of Fl-G4ori oligonucleotide was 90 ± 2 mA, which was significantly higher than that observed with oligo$(dT)_{25}$. Perhaps the higher anisotropy value is due to a somewhat larger size and rigid nature of this sequence, which is due to secondary structure unlike that observed with Fl-$(dT)_{25}$. The binding isotherm showed an initial plateau region due to free Fl-G4ori (Figure 2C) and increased with increasing concentrations of primase, leading to an increase in the extent of primase·Fl-G4ori complex formation (Figure 2C). The final anisotropy of the bound Fl-G4ori was ∼190 ± 3 mA. With both Fl-$(dT)_{25}$ and Fl-G4ori, saturation binding was reached above $(3.5 \pm 0.3) \times 10^{-7}$ M primase. Nonlinear regression analysis of the anisotropy data gave a K_d value of 1.22×10^{-7} M for Fl-G4ori. It is noteworthy that the dissociation constant for the CTG-containing G4ori sequence is somewhat lower than that observed with the Fl-$(dT)_{25}$ template. However, the difference between these two K_d values was small. The fluorescence intensity did not change during the titration, confirming that the quantum yield of the probe remained constant (Figure 2B,D).

Length and Sequence Dependence of DNA Binding by Primase. The binding affinities of oligonucleotides of varying length and sequences were tested by competition analysis as described in Materials and Methods. The primase·Fl-$(dT)_{25}$ complex was assembled using 2×10^{-7} M primase and

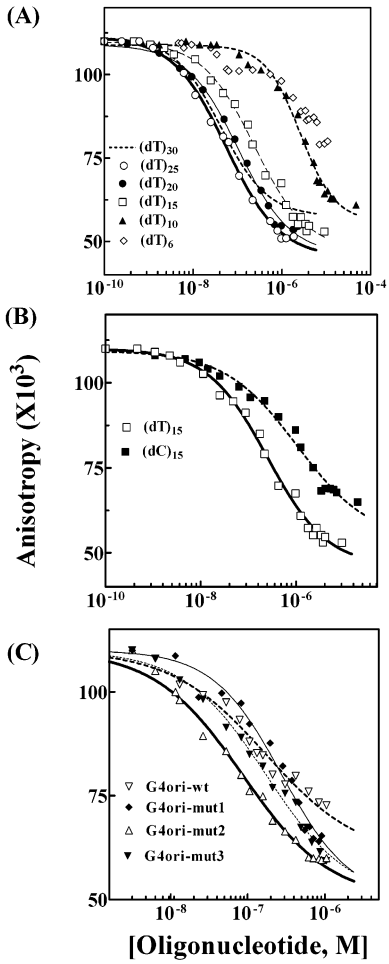

FIGURE 3: Inhibition of Fl-$(dT)_{25}$ binding by unlabeled oligonucleotides of different lengths and sequences. Titration of the preformed Fl-$(dT)_{25}$·primase complex with competitor oligonucleotides in buffer B containing 25 mM KCl: (A) $(dT)_{30}$ (- - -), $(dT)_{25}$ (○), $(dT)_{20}$ (●), $(dT)_{15}$ (□), $(dT)_{10}$ (▲), and $(dT)_6$ (◇), (B) $(dT)_{15}$ (□) and $(dC)_{15}$ (■), and (C) G4ori-wt (▽), G4ori-mut1 (◆), G4ori-mut2 (△), and G4ori-mut3 (▼). Nonlinear regression fits are represented with lines.

Table 2: Inhibition Constants of Unlabeled Oligonucleotides

oligonucleotide	K_i (M^{-1})	oligonucleotide	K_i (M^{-1})
$(dT)_{30}$	$(7.3 \pm 1.2) \times 10^{-8}$	$(dT)_{10}$	$(2.5 \pm 0.2) \times 10^{-6}$
$(dT)_{25}$	$(5.0 \pm 0.6) \times 10^{-8}$	$(dT)_6$	$>1.0 \times 10^{-5}$
$(dT)_{20}$	$(6.9 \pm 0.4) \times 10^{-8}$	G4ori-wt	$(8.7 \pm 0.3) \times 10^{-8}$
$(dT)_{15}$	$(1.9 \pm 0.3) \times 10^{-7}$	G4ori-mut1	$(2.8 \pm 0.3) \times 10^{-7}$
$(dC)_{15}$	$(6.0 \pm 0.9) \times 10^{-7}$	G4ori-mut2	$(8.2 \pm 0.7) \times 10^{-8}$
$(dA)_{15}$	ND[a]	G4ori-mut3	$(1.8 \pm 0.3) \times 10^{-7}$

[a] Not determined.

3×10^{-9} M Fl-$(dT)_{25}$, and the anisotropy of the complex was 110 ± 2 mA (Figure 3). Competition with unlabeled oligonucleotides displaced Fl-$(dT)_{25}$ from the complex, and the anisotropy decreased because of the formation of free Fl-$(dT)_{25}$.

Competition analysis for oligo(dT)s of varying lengths was carried out, and the data were analyzed by nonlinear least-squares regression (Figure 3A). In general, the apparent inhibition constants (K_i) increased with a decrease in the length of the oligonucleotides as indicated in Table 2. Both oligo$(dT)_{30}$ and oligo$(dT)_{20}$ demonstrated inhibition similar to that of oligo$(dT)_{25}$, suggesting that the binding was independent of length above 20 bp. The DNA binding affinity decreased significantly below 20 bp. The inhibition constant for oligo$(dT)_{15}$ was 3-fold higher than that obtained for oligo$(dT)_{25}$, whereas the K_i for oligo$(dT)_{10}$ was in the micromolar range. Smaller oligonucleotides, such as oligo$(dT)_6$, could not compete with Fl-$(dT)_{25}$ completely even at very high concentrations (Figure 3A). Our results demonstrated that the DNA binding affinity of primase depends on the length of the template, and it was optimal above 20 bp.

To evaluate the influence, if any, of nucleotide composition on DNA binding, we have compared oligo(dT) with oligo(dC). Oligo$(dC)_{15}$ was less efficient as a competitor of DNA binding than oligo$(dT)_{15}$ (Figure 3B), and K_i was significantly higher than that observed with oligo$(dT)_{15}$ (Table 2). The inhibition constants for oligo$(dC)_{15}$ and oligo$(dT)_{15}$ indicated that oligo$(dT)_{15}$ bound primase with a higher affinity than oligo$(dC)_{15}$. We have explored further the sequence dependence of primase by using wild-type G4 origin of replication (G4ori-wt) as well as G4ori templates mutated in the region of the semiconserved octanucleotide sequence 5′-CTGCAA-3′ (Table 1). These G4 sequences were used for competition against the Fl-$(dT)_{25}$·primase complex under similar conditions. A preformed complex of Fl-$(dT)_{25}$ and primase was challenged by titration with the G4ori-wt oligonucleotide. As shown in Figure 3C, G4ori-wt can effectively compete in primase binding and displace Fl-$(dT)_{25}$. Analysis of the competition data by nonlinear regression methods produced an inhibition constant of 8.7×10^{-8} M, which was comparable to that of oligo$(dT)_{30}$ (Table 2).

In G4ori-mut1, the well-conserved adenine was replaced with thymine. Analysis of the inhibition plot of G4ori-mut1 demonstrated that the inhibition constant ($K_i = 2.8 \times 10^{-7}$ M) was 3.5-fold higher than that for the wild-type sequence (Figure 3C and Table 2). As shown in Table 1, G4ori-mut2 was created by mutating CTG to CTT. Competition analysis with G4ori-mut2 indicated that the K_i (8.2×10^{-8} M) was similar to that observed with G4ori-wt (Table 2). Incidentally, CTT is also a preferred sequence for primase activity (*31*), which correlates well with the results of our binding studies. G4ori-mut3, where the CTG sequence was replaced with the TTG sequence (Table 1), exhibited an inhibition constant ($K_i = 1.8 \times 10^{-7}$ M) 2-fold higher than that of G4ori-wt (Table 2). The overall order for the primase affinity for these sequences is as follows: G4ori-wt ≈ G4ori-mut2 > G4ori-mut3 > G4ori-mut1. Comparable affinities of G4ori-mut2 and G4ori-wt for primase indicated that guanine in the CTG triplet is not essential for primase binding. Comparison of wild-type G4ori with G4ori-mut3 revealed that the cytosine in CTG is required for optimal binding to primase. Further analysis of G4ori-mut1 suggested that, in addition to the trinucleotide CTG sequence, the invariant adenosine in G4ori also plays a vital role in primase binding.

Temperature Dependence and Thermodynamic Parameters for DNA Binding by Primase. To delineate the thermodynamics of the primase−DNA binding interaction, we have analyzed primase binding with Fl-$(dT)_{25}$ and Fl-G4ori at several different temperatures: 23, 27, 30, 32, 37, and 42 °C. The binding isotherms for primase binding to Fl-$(dT)_{25}$ at different temperatures are presented in Figure 4, whereas the binding data for Fl-G4ori are not shown. Saturation DNA binding was observed at these temperatures for both Fl-$(dT)_{25}$

Table 3: Changes in K_d with Temperature

	23 °C	27 °C	30 °C	32 °C	37 °C	42 °C
$K_{d[Fl-(dT)_{25}]}$ ($\times 10^7$ M^{-1})	1.4 ± 0.05	1.34 ± 0.05	ND[a]	1.13 ± 0.05	0.9 ± 0.09	1.14 ± 0.05
$K_{d[Fl-G4ori]}$ ($\times 10^7$ M^{-1})	1.2 ± 0.08	ND[a]	1.1 ± 0.05	ND[a]	0.85 ± 0.08	1.12 ± 0.05

[a] Not determined.

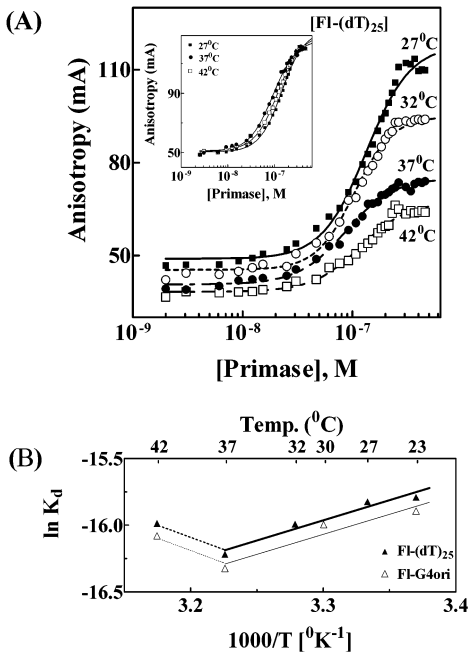

FIGURE 4: Temperature modulation of the primase−oligonucleotide interaction. (A) Titration of 3 nM Fl-$(dT)_{25}$ with primase at different temperatures in buffer B containing 25 mM KCl: 27 (■), 32 (○), 37 (●), and 42 °C (□). The inset shows normalized anisotropy data for the titration of Fl-$(dT)_{25}$ with primase at 27 (■), 37 (●), and 42 °C (□). The normalized plot for 32 °C overlapped with the plot for 27 °C and was, therefore, omitted. (B) van't Hoff analysis of the apparent dissociation constant (K_d) for the interaction of primase with Fl-$(dT)_{25}$ (▲) and Fl-G4ori (△) at different temperatures. Solid lines represent linear regression fits. Nonlinear regression fits are represented with dashed lines.

(Figure 4A) and Fl-G4ori templates. We observed an overall decrease in anisotropy values of the free and bound oligonucleotides with an increase in temperature. A similar decrease with temperature was observed with estrogen receptor binding to the estrogen responsive element, and the observed changes were due to a decrease in solvent viscosity with an increase in temperature (*27*). Therefore, the data for Fl-$(dT)_{25}$ were normalized (inset of Figure 4A). The dissociation constants of the primase·oligonucleotide complex decreased steadily with temperature between 23 and 37 °C (Table 3) for both sequences. The dissociation constant increased at 42 °C, probably due to the denaturation of the protein at this temperature. The primase·oligonucleotide complex was most stable at 37 °C and comparable for both Fl-$(dT)_{25}$ and Fl-G4ori.

We plotted the dissociation constants using the van't Hoff equation ($\ln K_d = -\Delta H°/RT$, where $\Delta H°$ is the enthalpy change and T and R are the temperature and gas constant, respectively) as shown in Figure 4B. For both oligonucleotide probes, the van't Hoff plot is linear up to 37 °C and deviated from linearity above 37 °C, which could be due to a conformational change in this temperature range. $\Delta H°$ was derived from the slope of the van't Hoff plot and was similar (−6.0 kcal/mol) for both oligonucleotides. The change in

Scheme 1. Three Possible Pathways of Primase Binding to Single-Stranded DNA that Were Analyzed

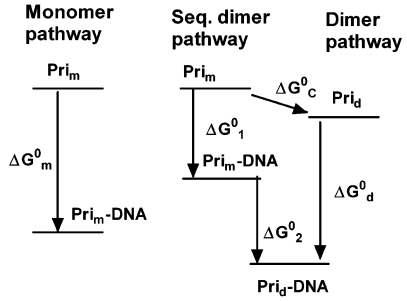

the entropy ($\Delta S°$) was calculated ($\Delta G° = -RT \ln K_d$ and $\Delta G° = \Delta H° - T\Delta S°$) and was found to be −51.6 cal K^{-1} mol^{-1}. Therefore, the DNA binding process is primarily entropy driven.

Primase Bound DNA as an Apparent Dimer. Primase exists as a monomer in solution even at a very high concentration (≥1 mg/mL) as determined by HPLC gel filtration chromatography (Figure 1). The Hill coefficients (n_{app}), obtained from the nonlinear regression of the binding isotherms of Fl-$(dT)_{25}$, was found to be 1.7. The Hill coefficient can be interpreted as the minimum number of monomers involved during complex formation (*32*). The Hill coefficient ($n_{app} = 1.7$) of these plots indicated that at least in this case, two primase monomers are binding DNA with a degree of cooperativity. Therefore, we have analyzed the binding isotherms further for determining possible modes of primase−DNA complex formation. We have considered several different possible models that could lead to the formation of the complex as shown in Scheme 1. Three pathways of primase·DNA complex assembly that were used to analyze the binding isotherms are presented in Scheme 1: (i) monomer binding model in which primase binds as a monomer and forms the Pri_m·DNA complex, (ii) sequential dimer binding model in which primase is first binding as a monomer to form the Pri_m·DNA complex followed by sequential association of a second monomer resulting in formation of the Pri_d·DNA complex, and (iii) dimer binding model in which primase forms a dimer before associating with single-stranded DNA (Pri_d·DNA).

The binding isotherm obtained by titration of Fl-$(dT)_{25}$ with primase in buffer B at 37 °C in the presence of 25 mM KCl was fitted to each of these three binding models, as shown in Figure 5A. The monomer binding model did not fit the binding isotherm or the dimer binding model. The sequential dimer model provided the best fit to the experimental binding data compared to the other models (Figure 5A). In addition, data from the residual fit showed more deviation from the baseline in the case of the monomer model than that observed with the sequential dimer model with a χ^2 value of 0.95 (Figure 5B). The sequential dimer model also fitted well with the binding isotherm obtained with the Fl-G4ori oligonucleotide (Figure 5C). These results revealed

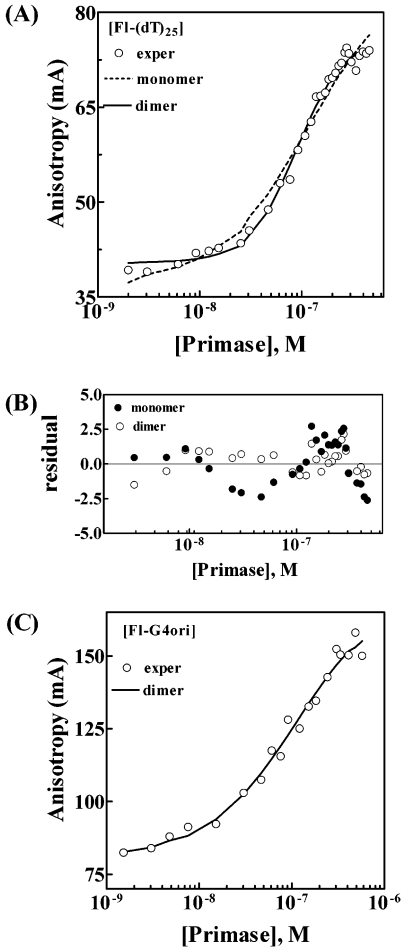

FIGURE 5: Binding models of the primase−oligonucleotide interaction by BIOEQS analysis. Panels A and C are the BIOEQS analyses of the anisotropy data obtained during the titration of 3 nM Fl-$(dT)_{25}$ and Fl-G4ori, respectively, with primase at 37 °C in buffer B containing 25 mM KCl. Solid and sequential dashed lines represent the sequential dimer and monomer fit, respectively. (B) Residuals obtained during the fit of the monomer (●) and dimer (○) data to the anisotropy data obtained during the titration of 3 nM Fl-$(dT)_{25}$ with primase at 37 °C.

that the sequential dimer model of stepwise binding of two primase monomers to the substrate DNA is the preferred pathway.

To further examine the various modes of primase·DNA complex formation, we have carried out an electrophoretic mobility shift assay (EMSA). Upon titration with primase, the migration of ssDNA was retarded, which clearly indicated the formation of the primase·DNA complex (Figure 6A). At lower primase concentrations, two closely spaced protein·DNA complex bands were observed which could be due to different modes of binding related to secondary structures of ssDNA. The plot of DNA concentration in femtomoles versus protein concentration in nanomolar (Figure 6B) revealed the K_d value of $(3.5 \pm 1.3) \times 10^{-7}$ M, which is comparable to that obtained from anisotropy measurements. The small difference is likely due to a difference in the two methodologies; in particular, the EMSA involves separation of the bound and free DNA that perturbs the equilibrium.

We also performed UV cross-linking of primase with DNA, where we could determine the molecular mass of the cross-linked products (Figure 7A,B). In the autoradiogram of the cross-linking gel, significant levels of two cross-linked

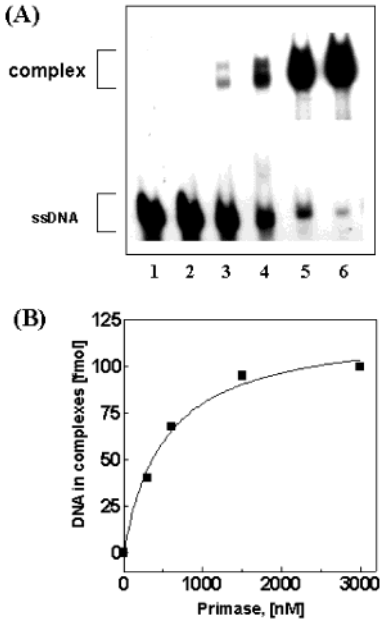

FIGURE 6: Analysis of the primase·ssDNA complex by gel retardation and a UV cross-linking assay. (A) The gel shift DNA binding assay was carried out as described in Materials and Methods with 1 ng of labeled G4ori-wt. Lane 1 represents labeled G4ori-wt alone, and lanes 2−6 represent labeled G4ori-wt with 0.25 (lane 2), 0.5 (lane 3), 1 (lane 4), 2.5 (lane 5), and 5 μg (lane 6) of primase, respectively. (B) Plot of bound DNA in femtomoles (fmol) vs primase concentration in nanomolar (nM). The solid line represents the nonlinear regression fit of the data.

bands were observed at ∼70 and ∼140 kDa for all primase concentrations (Figure 7B). These two species were found to have molecular masses consistent with that expected for complexes containing DNA cross-linked to the primase monomer (∼75 kDa) and the primase dimer (∼140 kDa), respectively. In addition to this, the dimer·DNA complex appeared to be more abundant than the monomer·DNA complex.

Energetics of Primase−DNA Binding. From the cooperative dimer fit, the free energy changes derived for the primase·Fl-$(dT)_{25}$ interaction were as follows: $\Delta G°_1 = -4.6$ kcal/mol for the monomer DNA interaction and $\Delta G° = -11.03$ kcal/mol for the overall association of two monomers to DNA, which were assigned to the formation of the Pri_m·Fl-$(dT)_{25}$ and Pri_d·Fl-$(dT)_{25}$ complexes, respectively. The free energy of cooperativity as defined by eq 11, $\Delta G°_c$, was found to be −1.8 kcal/mol. A low value indicated a weak interaction between the two monomers, which explained the lack of primase dimer formation in solution.

In the case of the CTG triplet containing the Fl-G4ori sequence, the cooperative dimer model revealed two free energy values: $\Delta G°_1 = -6.3$ kcal/mol and $\Delta G° = -11.7$ kcal/mol. Since in vivo and in vitro studies indicated that primase initiates primer synthesis preferably from CTG sequences and the calculated value of $\Delta G°_1$ for monomer binding to a non-CTG DNA sequence is 4.6 kcal/mol, we assigned the $\Delta G°_1$ value of −6.3 kcal/mol to primase monomer binding to the CTG-containing sequence in G4ori. The remaining free energy ($\Delta G°_2 = -5.4$ kcal/mol) is attributed to the binding interaction of the second monomer at the non-CTG site and cooperative interaction between the monomers. The cooperative free energy of the primase−primase interaction was −0.8 kcal/mol for Fl-G4ori.

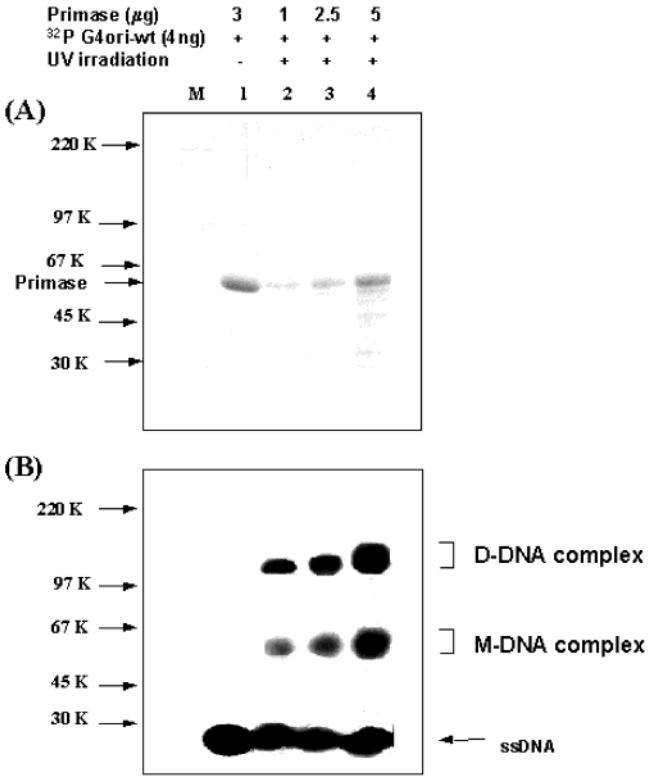

FIGURE 7: Photo-cross-linking of primase DNA complexes. UV cross-linking was performed as described in Materials and Methods. (A) Picture of a Coomassie blue R-250-stained SDS−PAGE gel. (B) Autoradiogram of the gel. During the experiment, ^{32}P labeled G4ori-wt was incubated with 3 (lane 1), 1 (lane 2), 2.5 (lane 3), and 5 μg (lane 4) of primase. Lane 1 represents an unirradiated primase·G4ori-wt complex. Lane M indicates the standard marker proteins, and their molecular masses are shown at the left side of the figure. In panel B, M and D refer to the primase monomer and primase dimer, respectively.

DISCUSSION

Primase is responsible for priming the entire *E. coli* genome during chromosomal DNA replication. Consequently, it has the ability to bind ssDNA regardless of sequence. However, it synthesizes primers at only certain sequences in a distributive manner. In the replication fork, it interacts with the DnaB helicase that unwinds DNA in a highly processive manner. Unlike transcription factors, such as the *trp* repressor or estrogen receptor, it is a mobile replication promoter and ssDNA passes through the DNA binding site at an extremely high rate. Therefore, the interaction of primase with ssDNA is certainly complex and dynamic. Although the roles of primase in replisome and lagging strand priming are well-established, the mechanism of its interaction with DNA remains to be understood.

Mechanism of DNA Binding by Primase. Primase appeared to bind a number of different single-stranded DNA templates, which is in accordance with its function in vivo. Therefore, to delineate the mechanism of the binding process, we have focused this study on two specific sequences. The apparent dissociation constants were determined for primase binding to (i) G4ori-wt, a CTG-containing template derived from bacteriophage G4 origin of DNA replication, and (ii) oligo-$(dT)_{25}$, a synthetic homopolymer sequence lacking the CTG triplet. The dissociation constant (K_d) for G4ori was found to be lower (1.2×10^{-7} M) than that observed with oligo-$(dT)_{25}$ (1.4×10^{-7} M), indicating a slightly higher binding affinity for the CTG-containing G4ori-wt sequence (Figure 2 and Table 1). The determination of K_d at different temperatures (23−42 °C) showed a uniform trend in K_d for both sequences. Therefore, the differences between the K_d values associated with these two oligonucleotide sequences are significant, even though the differences between the two sets were small. Our data also demonstrated that although primase bound DNA in the temperature range of 23−42 °C, the binding affinity of primase was highest at 37 °C, which is also the optimal temperature for *E. coli* growth. The free energy change for the primase−ssDNA interaction, determined from the van't Hoff plot to be −9.5 kcal/mol, was comparable to the free energy change computed for other DNA binding proteins (*33*). The van't Hoff analysis also revealed that the association of primase with ssDNA is primarily entropy driven. The structural analysis of primase indicates that the electropositive region of the NH_2-terminal subdomain provides a surface for the interaction with the DNA phosphodiester backbone, whereas the basic and the hydrophobic groups help to bind the RNA primer (*21*). Therefore, the favorable entropy of primase binding can be attributed to the release of water from the polar and nonpolar surfaces. The desolvation of polar groups contributes to the unfavorable enthalpy (*34*). Incidentally, we also determined that DNA binding is not influenced to a significant degree by ionic strength (data not shown).

Oligonucleotide Length and Sequence Dependence of Primase Binding. The DNA binding affinity of primase was found to be length- and sequence-dependent. Primase shows its highest binding affinity for templates ≥20 bases in length. The inhibition constant (K_i) was lower for oligo(dT) than that observed with oligo(dC), indicating that oligo(dT) is a better template than oligo(dC) for interaction with primase binding. Inhibition studies using G4ori and its mutants confirmed that the CT sequence of the d(CTG) recognition site was essential for efficient binding of primase with DNA. The increased K_i of G4ori-mut1 revealed that the invariant adenosine residue of G4 enhances the binding affinity of primase.

Primase Formed a 2:1 Complex with ssDNA. BIOEQS analysis of binding isotherms of primase−DNA binding showed that the stoichiometry of the primase−DNA complex was 2:1 as indicated by the fit of the data to a sequential dimer binding model. Further, gel retardation and UV cross-linking studies confirmed this model by demonstrating the formation of both primase monomer−DNA and dimer−DNA complex species.

The sequential dimer model demonstrated that the primase monomer bound oligo$(dT)_{25}$ with a ΔG°_1 of −4.6 kcal/mol. The free energy change for cooperativity was −1.8 kcal/mol. It is likely that this energy is involved in the primase−primase interaction. With the G4-ori sequence, ΔG°_1 for the first monomer is quite a bit higher (−6.3 kcal/mol) than that for the non-CTG sequence (−4.6 kcal/mol) such as oligo-$(dT)_{25}$. It was also higher than the ΔG°_2 for the second monomer binding. The first monomer bound the CTG site in G4ori, since primase has a higher affinity for the CTG trinucleotide (ΔG° = −6.3 kcal/mol), and the second monomer bound a non-CTG site.

Mechanism of Site Selection and Priming on the Lagging Strand. The X-ray crystal structure of primase shows that it

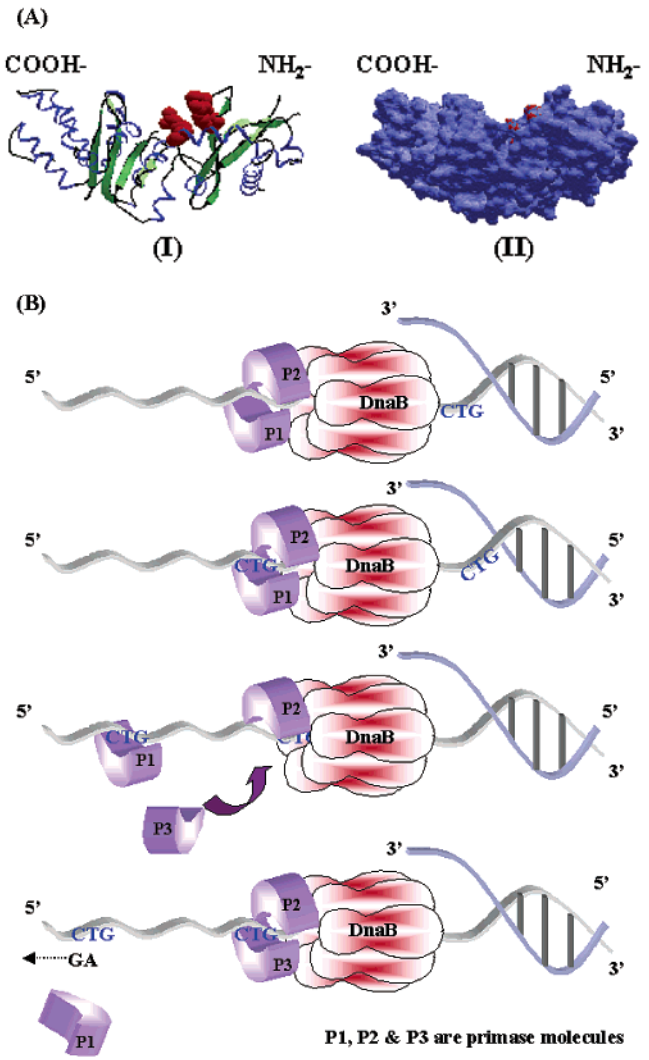

FIGURE 8: Model depicting primer synthesis by primase and DnaB helicase on the lagging strand of the replication fork. (A) X-ray crystal structure of the active site of *E. coli* primase that was reported by Keck et al. (*21*), shown as a ribbon model (I) and a hydrophilic surface model (II) displaying the putative DNA binding site and side chains (highlighted in red) involved in DNA binding: Arg146, Arg221, and Lys229. (B) Cartoon describing a proposed model of the roles of primase and DnaB helicase in site selection and priming of lagging strand DNA replication in *E. coli*. The bound DNA is ssDNA oriented in the 5′ to 3′ direction. P1−P3 are primase molecules. CTG represents the recognition and primer synthesis initiation sites.

has a sickle-shaped structure with a shallow, wedge-shaped cleft on the concave side of the protein as shown in Figure 8A (*21*). Keck et al. (*21*) proposed that the ssDNA threads through the cleft, which is supported by the electropositive ridge of the NH_2 subdomain. We have developed a putative model of primase actions based on the sequential dimer binding model, free energy changes involved in each monomer binding, as described here, and the sickle-shaped X-ray crystal structure of the primase molecule with only one Zn finger DNA binding domain (Figure 8B). In this model, two primase monomers interact with the DnaB helicase and bind to DNA (Figure 8B). In Fl-G4ori, one monomer bound to the CTG sequence and the second monomer was likely associating on the opposite side. Consequently, primase binds to DNA more tightly upon encountering a CTG triplet during replication that possibly acts as a trigger for initiation of primer synthesis. Primase has distributive action (*11*), and therefore, it dissociates from the template DNA after forming the primer (Figure 8B). This may be due to the free energy difference between monomer and dimer binding. After initiation of the priming event on CTG, it will be difficult for the primase to stay attached to DNA for an extended duration as a monomer. This duration of binding could be just long enough for synthesis of a small primer and complete dissociation from the template upon completion of primer synthesis (Figure 8B).

During replication, ssDNA passes through the primase DNA binding site at the rate of ~1000 nucleotides per second. This rate is feasible only when there is no significant sequence dependence. We have proposed that a slightly greater binding affinity for CTG-containing sequences will result in (i) dissociation of primase from the primosome, (ii) initiation of primer synthesis at the CTG sequence, (iii) dissociation of the primase from the lagging strand at the culmination of primer synthesis, and (iv) association of a new primase molecule with the primase site in the primosome as depicted in Figure 8B. This model of primase action holds that the concentration of primase will determine how long the primase site remains vacant in the primosome, the frequency of lagging strand priming, and the lengths of the Okazaki fragments. During the period of the absence of primase from the primosome, another CTG sequence will pass through the primosome without being primed. Therefore, the relative distance between the primers as well as the lengths of the Okazaki fragments would be inversely proportional to the primase concentration.

The sequential dimer model that we have proposed in Figure 8B is also supported by the structural requirements of Zn finger DNA binding proteins. DNA binding proteins of this class normally have two zinc fingers, which fit into the major groove of the DNA double helix (*35*). Primase, on the other hand, has only one N-terminal zinc finger motif (*36*), which may not be sufficient for the formation of a stable primase·DNA complex that agrees well with the thermodynamic data presented here. Therefore, a second primase molecule is required to provide one more zinc finger site and to form a stable DNA·protein complex. Together, the two primase monomers form a stable complex with DNA without actually forming a true stable dimer. In addition, this model does not preclude formation of higher-order protein·DNA complexes, beyond a 2:1 primase·DNA complex, in the presence of DnaB helicase.

ACKNOWLEDGMENT

We thank Dr. Richard H. Ebright of Waksman Institute, Rutgers University, for critically reviewing the manuscript; Dr. Roger McMacken of Johns Hopkins University for the gift of the pRLM96 plasmid containing the wild-type DnaG/primase gene; Dr. Catherine A. Royer (Centre de Biochimie Structurale, INSERM, Montpellier, France) for the gift of BIOEQS software and training involving data analysis; and Mr. Stephen J. Flowers of this laboratory for help with modeling studies and computer graphics.

REFERENCES

1. Kornberg, A., and Baker, T. A. (1992) Primases, Primosomes and Priming, in *DNA Replication*, 2nd ed., W. H. Freeman & Co., New York.

2. van-der Ende, A., Baker, T. A., Ogawa, T., and Kornberg, A. (1985) *Proc. Natl. Acad. Sci. U.S.A. 82*, 3954−3958.
3. DePamphilis, M. L. (1993) *Annu. Rev. Biochem. 62*, 29−63.
4. Frick, N. D., and Richardson, C. C. (2001) *Annu. Rev. Biochem. 70*, 39−80.
5. Arai, K., and Kornberg, A. (1981) *J. Biol. Chem. 256*, 5267−5272.
6. Rowen, L., and Kornberg, A. (1978) *J. Biol. Chem. 253*, 758−764.
7. Fiddes, J. C., Barrell, B. G., and Godson, G. N. (1978) *Proc. Natl. Acad. Sci. U. S. A. 75*, 1081−1085.
8. Kitani, T., Yoda, K., Ogawa, T., and Okazaki, T. (1985) *J. Mol. Biol. 184*, 45−52.
9. Yoda, K., and Okazaki, Y. (1991) *Mol. Gen. Genet. 227*, 1−8.
10. Wu, C. A., Zechner, E. L., and Marians, K. J. (1992) *J. Biol. Chem. 267*, 4030−4044.
11. Zechner, E. L., Wu, C. A., and Marians, K. J. (1992) *J. Biol. Chem. 267*, 4045−4053.
12. Swart, J. R., and Griep, M. A. (1995) *Biochemistry 34*, 16097−16106.
13. Bouche, J. R., Zechel, K., and Kornberg, A. (1975) *J. Biol. Chem. 250*, 5995−6001.
14. Yarranton, G. T., Das, R. H., and Gefter, M. L. (1979) *J. Biol. Chem. 254*, 11997−12001.
15. Seki, M., Enomoto, T., Watanabe, Y., Tawarag, Y., and Kawasaki, K. (1986) *Biochemistry 25*, 3239−3245.
16. Chao, K., and Lohman, T. (1991) *J. Mol. Biol. 221*, 1165−1181.
17. Finger, L. R., and Richardson, J. P. (1982) *J. Mol. Biol. 156*, 203−219.
18. Lee, J., Tonozuka, T., and Jayaram, M. (1997) *Genes Dev. 11*, 3061−3071.
19. Kim, K., Namgoong, S. Y., Jayaram, M., and Harshey, R. M. (1994) *J. Biol. Chem. 270*, 472−479.
20. McMacken, R., Ueda, K., and Kornberg, A. (1977) *Proc. Natl. Acad. Sci. U.S.A. 74*, 4190−4194.
21. Keck, J. L., Roche, D. D., Lynch, A. S., and Berger, J. M. (2000) *Science* 287, 2482−2486.
22. Stayton, M., and Kornberg, A. (1983) *J. Biol. Chem. 258*, 13205−13212.
23. Lakowicz, J. R. (1999) *Principles of fluorescence spectroscopy*, 2nd ed., Plenum Publishers, New York.
24. Mullaney, J. M., Thompson, R. B., Gryczynski, Z., and Black, L. W. (2000) *J. Virol. Methods 88*, 35−40.
25. Heyduk, T., Ma, Y., Tang, H., and Ebright, R. H. (1996) *Methods Enzymol. 274*, 492−503.
26. Ozers, M. S., Hill, J. J., Ervin, K., Wood, J. R., Nardulli, A. M., Royer, C. A., and Gorski, J. (1997) *J. Biol. Chem. 272*, 30405−30411.
27. Boyer, M., Poujol, N., Margeat, E., and Royer, C. A. (2000) *Biochemistry 28*, 2494−2502.
28. Royer, C. A., Smith, W. R., and Beecham, J. M. (1990) *Anal. Biochem. 92*, 287−294.
29. Bradford, M. M. (1976) *Anal. Biochem. 72*, 248−254.
30. Biswas, S. B., and Kornberg, A. (1984) *J. Biol. Chem. 259*, 7990−7993.
31. Bhattacharya, S., and Griep, M. A. (2000) *Biochemistry 39*, 745−772.
32. Kelley De Zutter, J., and Knight, K. L. (1999) *J. Mol. Biol. 293*, 769−780.
33. Jan-Jakobson, L., Engler, Z. E., Ames, J. T., Kurpiewski, M. R., and Grigorescu, A. (2000) *Structure* 8, 1015−1023.
34. Sharp, K. A. (1995) *Biopolymers 36*, 227−243.
35. Klug, A., and Schwabe, J. W. (1995) *FASEB J. 9*, 597−604.
36. Ilyina, T. V., Gorbalenya, A. E., and Koonin, E. V. (1992) *J. Mol. Evol. 34*, 351−357.

BI026711M